JETIR.ORG ISSN: 2349-5162 | ESTD Year : 2014 | Monthly Issue
JOURNAL OF EMERGING TECHNOLOGIES AND INNOVATIVE RESEARCH (JETIR)
An International Scholarly Open Access, Peer-reviewed, Refereed Journal

Investigating the Mechanical Properties of High-Strength Fiber-Reinforced Concrete: A Focus on Glass and Steel Fibers

Ambeshwar Singh Bhadauria
Construction Technology & Management
Department of Civil Engineering
Madhav Institute of Technology & Science
Gwalior, India

Gautam Bhadoriya
Department of Civil Engineering
Madhav Institute of Technology & Science
Gwalior, India

***Abstract*—Most of the existing research is based on reinforcement of concrete using steel and glass fibers only. A compression test was used to examine the strength of the reinforced concrete, tensile test. The self-compacting concrete lacks adequate compaction which deteriorates its compressive strength. It is therefore essential to augment its strength which could be achieved by addition of high-strength fibers. The current research is intended to enhance the strength of concrete using high-strength fibers. The structural characteristic of reinforced concrete would then be evaluated using compressive test and tensile test. Glass fibre reinforced concrete with a 0.3% fibre content has a compressive strength of 21.8N/mm2. The compressive strength obtained for glass fiber-reinforced concrete with 0.5% fiber content is 27.9N/mm2. With a fibre percentage of 0.3 percent, steel fiber-reinforced concrete achieves a compressive strength of 27.7N/mm2. Steel fibre reinforced concrete with a 0.5% fibre content has a compressive strength of 23.5N/mm2. The FEA simulation is conducted to determine the normal stresses and deformation of glass fiber specimen at different loads. From the FEA analysis on glass fiber specimen, the maximum normal stress obtained at 492kN is 19.903MPa. This is obtained for glass fiber percentage of 0.3%.**

Keywords—Self-compacting concrete, FEA, tensile test.

I. INTRODUCTION

Concrete is a highly regarded material in the construction industry and has been extensively utilised for well over a century. More and more issues might arise from inadequate compaction of concrete and from the incorrect filling of the systems in reinforced concrete buildings as the formworks and reinforcement become more sophisticated and exceedingly thick. Because of this, mature concrete's durability and performance may suffer. The enhancement of concrete's durability and working conditions has been given high priority in the evolution of concrete construction. As a result, SCC has gained popularity because of its higher quality and greater endurance without the need for compaction. Increased efficiency and the ability to cast homogenous concrete in confined spaces were two of the many ways in which this innovation revolutionised the concrete industry. Invented in Japan in 1986, SCC is a kind of concrete that doesn't need external compaction during the pouring process but entirely fills the formwork and flows through complicated geometrical designs and severely reinforced sections. In addition to these gains, the construction industry also stands to gain greatly from SCC's many other benefits, such as improved productivity on-site through decreased labour costs and construction times, freedom from noise pollution & health concerns related to vibration apparatus, and the generation of superior surface finishes with fewer faults.

It is generally agreed that SCC must satisfy all three of the following conditions: passage ability, filling ability, and segregation resistance. To meet these demands, a well-planned method of designing SCC mixture proportions is necessary; nevertheless, the tension between high fluidity & stability makes SCC more difficult to design than vibrated concrete. There is a pressing need to create a mix design approach for proportioning SCC mixes so that adequate qualities of fresh concrete may be obtained that meet the self-compatibility standards since no uniform mix design strategy has been employed so far. It is generally accepted that the concrete's fracture behaviour governs the collapse of concrete buildings and allows for the strength of fractured structures to be assessed. Fracture mechanics provides an energy-based failure theory which may be used in the design of cement-based structures by analysing their reactions & failures due to crack initiation and propagation. The specific fracture energy & stress-crack relationship are the most crucial parameters for defining the fracture behaviour of the concrete mixture. Concerns concerning the fracture behaviour and, by extension, the cracking processes of SCC have been highlighted by researchers because of the differences in SCC and VC composition. In addition, there is an urgent requirement for a study of the fracture behaviour of SCC since so little research has been done on its fracture characteristics.

The rheological properties of freshly mixed SCC have a significant impact on its workability and performance during placement, which includes transportation and pumping. The attributes of the final mix are affected by the quality of the individual components used to make it. Important characteristics of SCC include its capacity to flow across restricted and constrained areas, such as getting past obstructions and filling the formwork. It is critical to understand and predict the flow characteristics of the SCC mix in restricted areas or around obstacles such as Lbox in order to analyse how SCC fills work parts as a homogeneous mass without the segregation of mix components. The best approach to learn this is via numerical simulations, which will show where the bigger aggregate particles are located inside the formworks and provide information on the flow behaviour of SCC.

A. Contribution of this paper

The current research is intended to enhance the strength of concrete using high-strength fibers. The structural characteristics of reinforced concrete would then be evaluated using compressive tests and tensile tests. The detailed contributions are:

- Preparation of self-compaction concrete without fibers
- Structural assessment of self-compacting concrete (without fibers) using compressive test, tensile test.
- Preparation of self-compaction concrete with steel fibers and glass fiber.
- Structural assessment of self-compacting concrete (with fibers) using compressive test, tensile test.
- FEA structural analysis of fiber-reinforced concrete using ANSYS simulation package.

B. Organized of this paper

The rest of the paper is organized as follows: **Section II** describes some previous work of compacting concrete. **Section III** explains the methodology, and the experimental results are presented and analyzed in **Section IV**. Finally, the conclusions are drawn in **Section V**.

II. Literature Review

In this section, provide some related work of the study for self-compacting concrete.

Aslani et. al. Lightweight aggregates like crumb rubber or scoria are being studied in conjunction with recycled concrete aggregates to better understand the hardened and fresh features of different kinds of SCC. Tests for freshness including the T500, slump flow, and J-ring were conducted. Recycled cement and rubber crumb aggregates SCC are examined for their optimal design in the context of streamlining the development of new properties. The recommended SCC mixture has the potential to cut the amount of recycled concrete in half [1].

Djamila et. al. The Compressive Strength assessments were predicted using a pattern recognition neural network approach based on inputs including the amount of water present, the type of mineral admixture, the amount of cement present, the level of mineral admixture substitution for cement by weight, the tensile strength, the slump flow, the sieve segregation resistance, and the L-box [2].

Keshavarz et. al. Most studies of SCC have focused on its mechanical or rheological qualities or its durability. The cement's microstructural characteristics were studied. The study's findings showed that incorporating Nano silica (NS) and reinforcing fibre into SCC at optimal rates may improve the material's durability and mechanical properties [3].

Beigi et. al. Concrete's CS is widely regarded as an important mechanical feature and the primary mechanical parameter in determining the kind of concrete that is produced. They investigate nuanced methods of figuring to ascertain the CS in the concrete. To be more specific, after 28 days of water curing, the CS was determined for 150 samples of concrete with varying mix structure parameters. The results proved that both the ANN and Adaptive NeuroFuzzy Inference System (ANFIS) models were successful in predicting the CS. Furthermore, the outcomes showed that ANFIS is considerably more skillful than ANN in predicting concrete CS [4].

Alsubari et. al. At 30%, 20%, 10%, and 0%, sustainable SCC was produced by replacing concrete with Modified Treated Palm Oil Fuel Ash (MT-POFA). The results of the tests showed that the fresh characteristics of MT-POFA-containing concrete fell within the range expected in SCC. While MT-POFA cements showed a decline in mechanical qualities in the early curing stages, these features might be improved upon by allowing for a longer curing period. When tested against the control SCC, the one that included MT-POFA proved to be much more effective at high temperatures. As a cement substitute, MT-POFA performed well in the SCC [5].

A. Research gaps

There are significant knowledge gaps that must be filled in the area of self-compacting concrete (SCC) research. Extensive research on the sustainability and performance implications of lightweight aggregates mixed with recycled materials, such as crumb rubber, scoria, and MT-POFA, is necessary. To evaluate the additives' long-term effects and ecological footprint, it is essential to comprehend how they combine with other SCC components. Further, although prediction models such as Adaptive NeuroFuzzy Inference System (ANFIS) and Artificial Neural Networks (ANN) have been developed to estimate compressive strength (CS), it is critical to enlarge these models to forecast other mechanical characteristics and study the impacts of different admixtures and curing circumstances. Improving SCC's workability, strength, and durability also requires optimising mix design parameters including water-to-cement ratio, superplasticizer dose, and aggregate size. It's also important to compare various aggregate shapes and sizes. Filling these gaps will help produce more sustainable and high-performance SCC formulations, which will lead to their wider use in building.

III. Methodology

In this section, provide the methodology that is utilized for the proposed techniques.

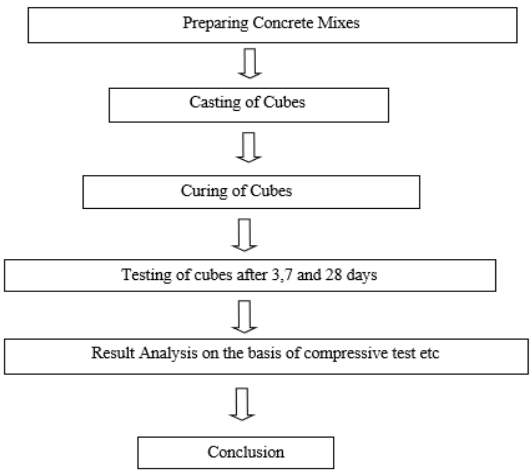

Fig. 1. Proposed flowchart

A. Preparation of Concrete Cube Specimen

These concrete test samples are made with the same proportions and material as real-world applications.

1) Mixing of Concrete for Cube Test

Use a hand or laboratory batch mixer to combine the concrete ingredients.

- On top of a waterproof, non-absorbent foundation, a uniformly coloured mixture of cement and fine aggregate should be laid.
- Once the cement and fine aggregate have been well mixed, it is time to add the coarse aggregate.
- Mix in water and continue stirring until the concrete seems uniform and the right consistency is reached.

2) Sampling of Cubes for Test

- Remove debris and grease the mounds.
- Pour concrete into moulds to a depth of about 5 centimetres.
- Use a tamping rod and make at least 35 strokes into each layer to compact it.
- Make the top layer even and smooth using a trowel

3) Curing of Cubes

Following the test samples have been maintained in humid air for 24 hours, they are labelled and taken out of the moulds, after which they are kept immersed in clear freshwater until it is time to conduct the test.

B. Slump Test (Procedure)

- A frustum of a cone 300 mm in height is used as the "concrete slump test mould" (12 in). The top opening is 100 mm (3.9 in) and the bottom is 200 mm (8 in) in diameter (4 in).
- After the concrete has been mixed, the container is filled three times before the base is set on a flat surface to see whether it is workable.
- In order to heat each layer 25 times, a steel rod measuring 16 mm (5/8 in) at its thickest point is employed.
- When the concrete has reached the top of the mould, the temping rod is rolled and screened to remove the excess material.
- Grips or foot-rests brazed to the mould are used to keep it firmly affixed to its base during the whole process, preventing it from shifting while the concrete is poured.
- After the cone has been filled and levelled with concrete, it is lifted vertically. Unsupported concrete will sink.
- Concrete that has been allowed to droop has lost height in the middle.
- When determining the slump, the cone is set up close to the depressed concrete, and the temping rod is set up above the cone in a way that allows it to pass through the slumped concrete.
- The mould is taller than the concrete when compared at the same scale. To the nearest 5 mm (1/4 in) is how most measurements are made [6].

C. Compressive Strength Test

- The cubes used in this test are mostly 150mm * 150mm * 150mm.
- The mounds are cleaned before application of oil to frame
- Filling of moulds with concrete layer of 50mm thickness. Compacting of layer with nearly 35 strokes using steel bar.
- Smoothing of top surface using trowel.
- Removal of concrete cubes from moulds within 72hrs.
- The specimen is removed from water after stipulated time
- The specimen is set in the machine and loads are applied to the cube in opposite directions.
- Alignment of the specimen at the center of base plate of machine.
- The movable piece is rotated gently in order to touch the top surface of specimen.
- Gradual application of load in steps of 140 kg/cm2/min. The load is applied in small increments till the specimen breaks.
- Documenting the maximum load required for breakage.

D. Problem Definition

Most of the existing research is based in reinforcement of concrete using steel and glass fibers only. The reinforced concrete was tested using compression test, tensile test. The self-compacting concrete lacks adequate compaction which deteriorates its compressive strength. It is therefore essential to augment its strength which could be achieved by addition of high-strength fibers. These fibers include steel fibers, glass fibers.

IV. Results & Discussions

This section provide the various output of the study in the form of table and figures.

A. Experimental Results on Glass fiber

The compressive test is conducted on M20-grade concrete with glass fiber. The specimen is prepared at Kalinga University Lab located at Raipur. The specimen composition is given below:

TABLE I. Composition of glass fiber concrete

Material	Proportion In Kg	Ratio
Cement	50 KG	1
Sand	75 KG	1.5
Agg. 20 Mm	150 KG	3
Fiber	825 G / 1.37 KG	0.3% / 0.5 %
Superplasticizer	2.75 L	1
Water	28 L	

Figure 5.5: Compressive strength test on casted cube

TABLE II. Glass fiber results

M20 (0.3 %)			
BLOCK	LOAD (KN)	LOAD (KG)	STRESS = LOAD/AREA
28 DAY	492	49200	21.8 N/SQ.MM
M20 (0.5%)			
28 DAY	628	62800	27.9 N/SQ.MM

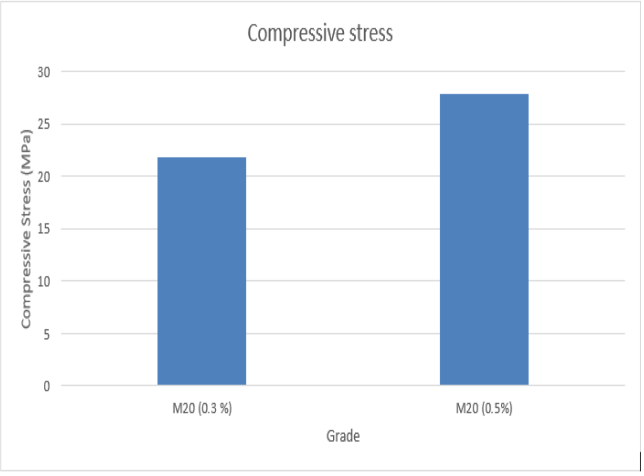

Fig. 2. Compressive Strength comparison for glass fiber concrete

TABLE III. STEEL FIBER RESULTS

M20 (0.3 %)			
BLOCK	LOAD (KN)	LOAD (KG)	STRESS = LOAD/AREA
28 DAY	625	62500	27.7 N/SQ.MM
M20 (0.5 %)			
28 DAY	530	53000	23.5 N/SQ.MM

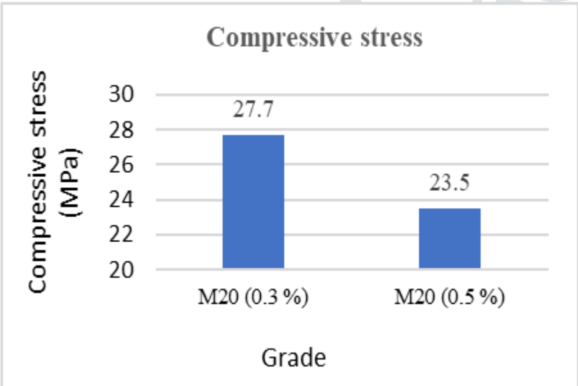

Fig. 3. Compressive Strength comparison for steel fiber

B. *Experimental Results on Steel fiber*

TABLE IV. STEEL FIBER RESULTS

M20 (0.3 %)			
BLOCK	LOAD (KN)	LOAD (KG)	STRESS = LOAD/AREA
28 DAY	625	62500	27.7 N/SQ.MM
M20 (0.5 %)			
28 DAY	530	53000	23.5 N/SQ.MM

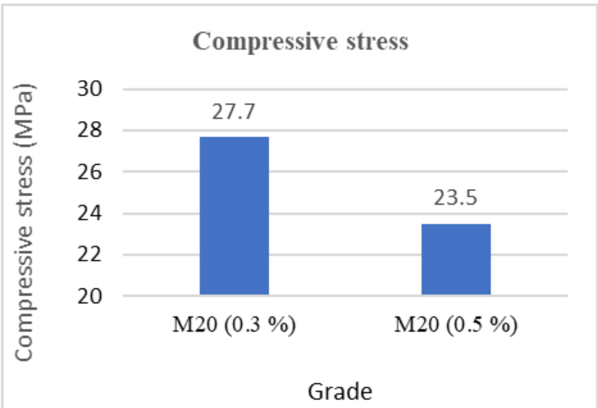

Fig. 4. Compressive Strength comparison for steel fiber

C. *Experimental Results on L Box test*

Self-compacting concrete's cohesiveness and flowability are evaluated using the L-Box test according to BS EN 12350-10.

- Two (59 ± 1mm space) or 3 bar tests
- (41 ± 1mm space)
- Fill the hopper and hit the ground.
- Stand for 60 ± 10sec
- Wait for traffic to halt before opening the gate.
- The horizontal to vertical depth ratio is known as the passing ability ratio (PL).

TABLE V. L BOX RESULTS

Passing Ratio (H1)	Blocking Ration (H2)	Passing Ability Pa= H2/H1
138 MM	122 MM	0.88
132 MM	119 MM	0.90
142 MM	120 MM	0.84

1) *FEA Simulation*

In this section, the structural analysis is conducted on M20 cube with glass fiber and steel fiber. The structural analysis is conducted using ANSYS simulation package. The FEA simulation involves CAD modeling, meshing, loads/boundary conditions, solution, and post-processing.

TABLE VI. GLASS FIBER 3% PROPERTIES

Modulus of Elasticity	25GPa
Poissons ratio	.18
Density (Kg/m3)	2200

TABLE VII. GLASS FIBER 5% PROPERTIES

Modulus of Elasticity	28GPa
Poissons ratio	.19
Density (Kg/m3)	2250

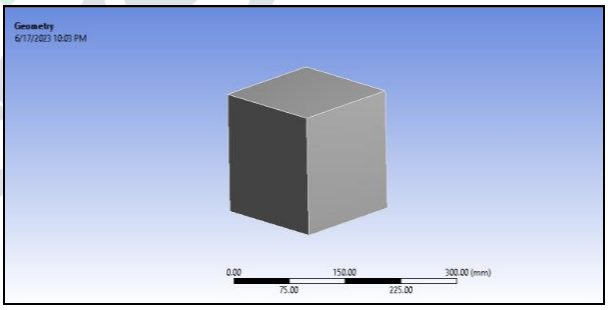

Fig. 5. CAD Design of specimen

The CAD model of specimen is developed in ANSYS design modeler. The dimensions of specimen are 150mm*150mm*150mm. The CAD model is meshed using shape elements as shown in figure 5.6. The model of specimen is meshed using fine sizing.

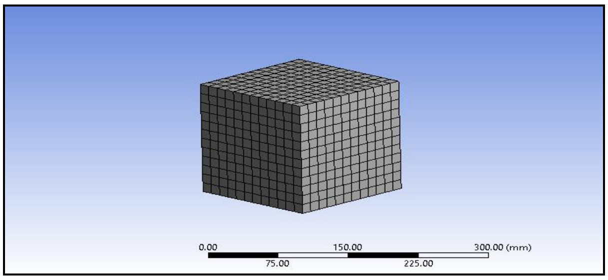

Fig. 6. Meshed model of specimen

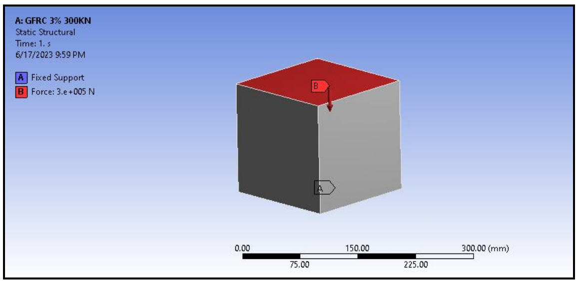

Fig. 7. Loads and Boundary Conditions

After meshing, the structural loads and boundary conditions are applied on the specimen as shown in Figure 5.7 above. The force of 300kN, 350kN, 400kN, 450kN and 492kN. The analysis is conducted for both glass fiber and steel fiber concrete.

2) Glass Fiber Reinforced Concrete Results with 3% Glass Fiber Content

The FEA analysis results are obtained for GFRC with 3% fiber concrete at different loads i.e. 300kN, 350kN, 400kN, 450kN, and 492kN.

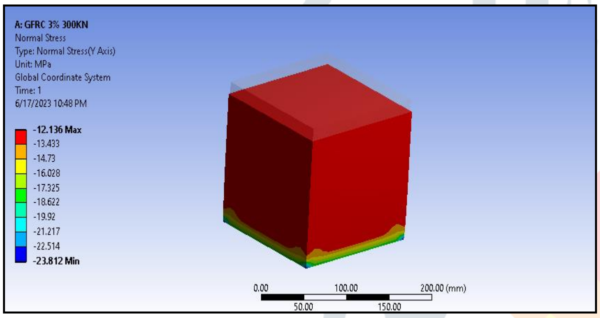

Fig. 8. Normal stress induced on GFRP specimen at 300KN load

The normal stress distribution plot is obtained for GFRP specimen at 300kN. The maximum normal stress obtained from the analysis is 12.13MPa as shown in figure 5.8.

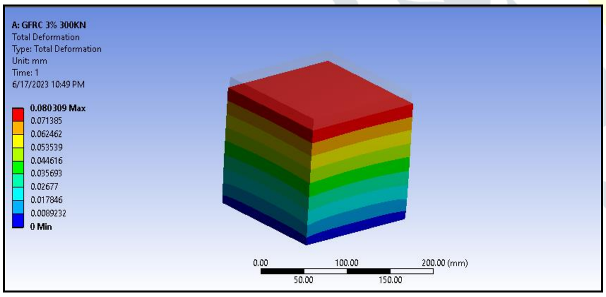

Fig. 9. Total deformation plot on GFRP specimen at 300KN load

The maximum deformation obtained on GFRP specimen at 300kN is .08mm as shown in Figure 5.9.

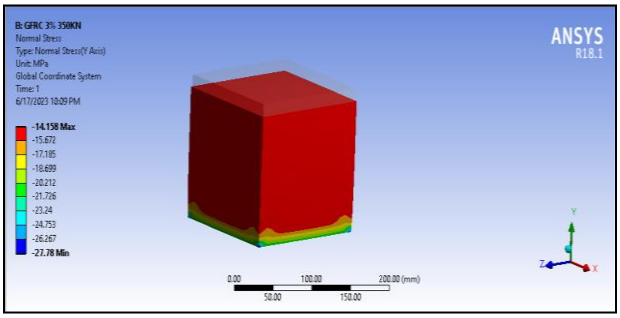

Fig. 10. Normal stress induced on GFRP specimen at 350KN load

The normal stress distribution plot is obtained for GFRP specimen at 350kN. The maximum normal stress obtained from the analysis is 14.15MPa as shown in figure 5.10.

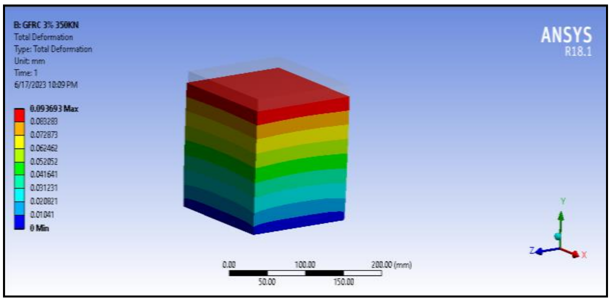

Fig. 11. Deformation induced on GFRP specimen at 350KN load

The maximum deformation obtained on GFRP specimen at 350kN is .093mm.

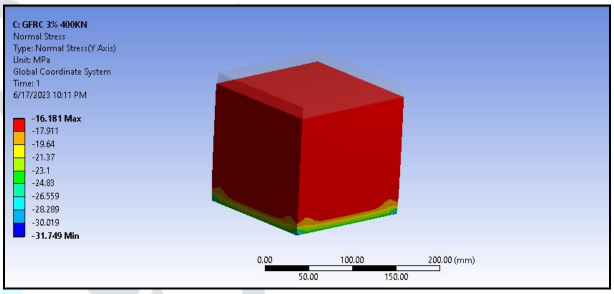

Fig. 12. Normal stress induced on GFRP specimen at 400KN load

The normal stress distribution plot is obtained for GFRP specimen at 400kN. The maximum normal stress obtained from the analysis is 16.18MPa as shown in figure 5.12.

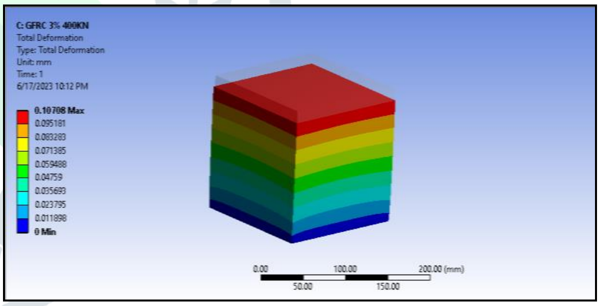

Fig. 13. Deformation induced on GFRP specimen at 400KN load

The maximum deformation obtained on GFRP specimen at 400kN is .107mm.

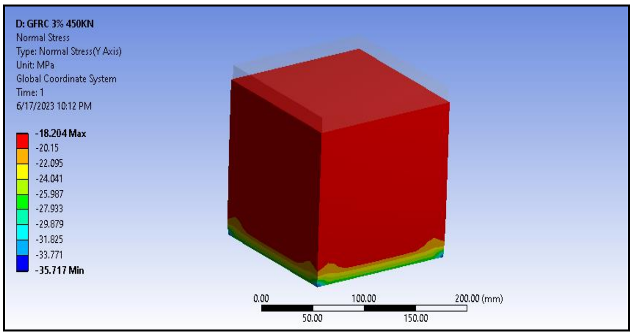

Fig. 14. Normal stress induced on GFRP specimen at 450KN load

The normal stress distribution plot is obtained for GFRP specimen at 450kN. The maximum normal stress obtained from the analysis is 18.204MPa as shown in figure 5.14.

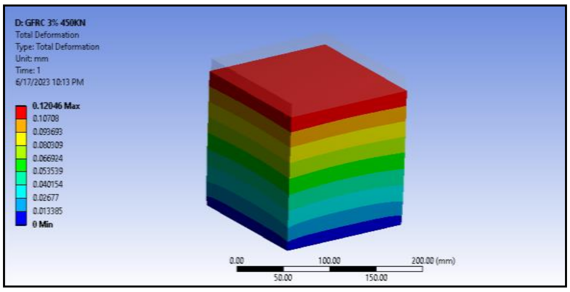

Fig. 15. Deformation induced on GFRP specimen at 450KN load

The maximum deformation obtained on GFRP specimen at 450kN is .107mm.

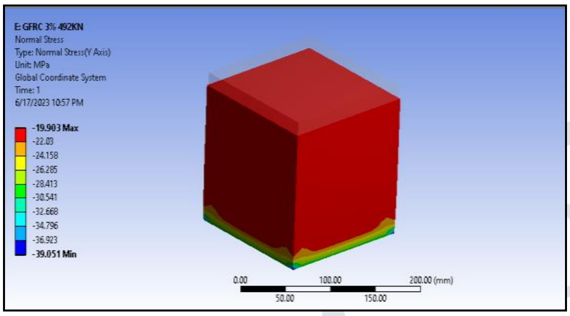

Fig. 16. Normal stress induced on GFRP specimen at 492KN load

The normal stress distribution plot is obtained for GFRP specimen at 492kN. The maximum normal stress obtained from the analysis is 19.903MPa as shown in figure 5.16.

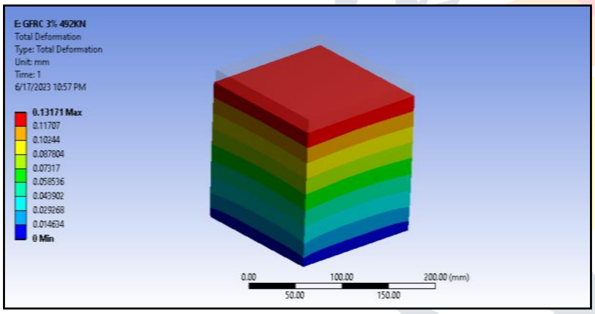

Fig. 17. Deformation induced on GFRP specimen at 492KN load

The maximum deformation obtained on GFRP specimen at 492kN is .131mm.

3) Glass Fiber Reinforced Concrete Results with 5% Glass Fiber Content

The FEA analysis results are obtained for GFRC with 3% fiber concrete at different loads i.e. 550kN, 600kN, and 628kN.

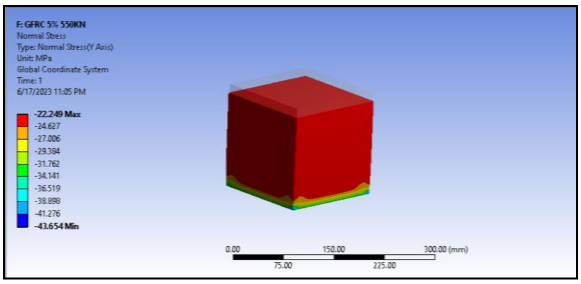

Fig. 18. Normal stress induced on GFRP specimen at 550kN load

The normal stress distribution plot is obtained for GFRP specimen at 550kN. The maximum normal stress obtained from the analysis is 22.24MPa as shown in figure 5.18.

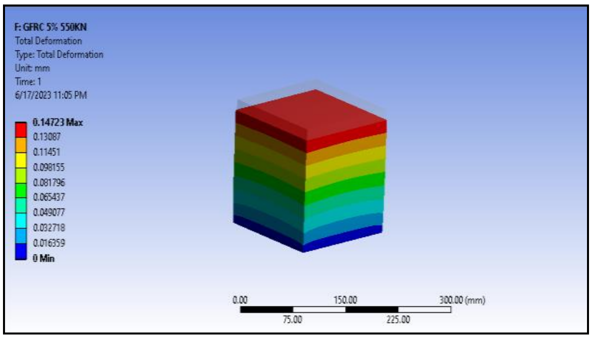

Fig. 19. Total deformation on induced on GFRP specimen at 550kN load

The maximum deformation obtained on GFRP specimen at 550kN is .147mm.

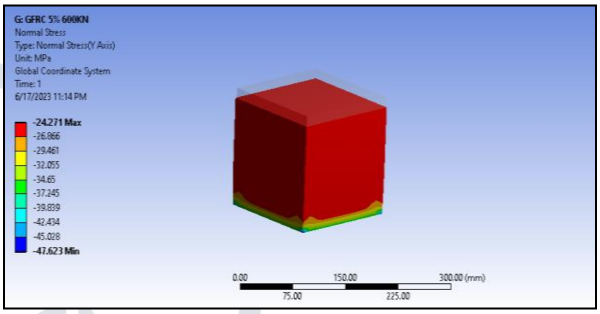

Fig. 20. Normal stress induced on GFRP specimen at 600kN load

The normal stress distribution plot is obtained for GFRP specimen at 600kN. The maximum normal stress obtained from the analysis is 24.27MPa as shown in figure 5.20.

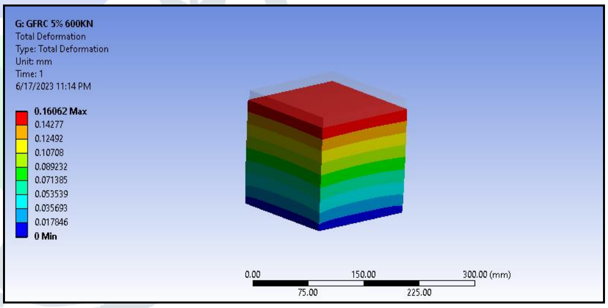

Fig. 21. Total deformation on induced on GFRP specimen at 600kN load

The maximum deformation obtained on GFRP specimen at 600kN is .160mm.

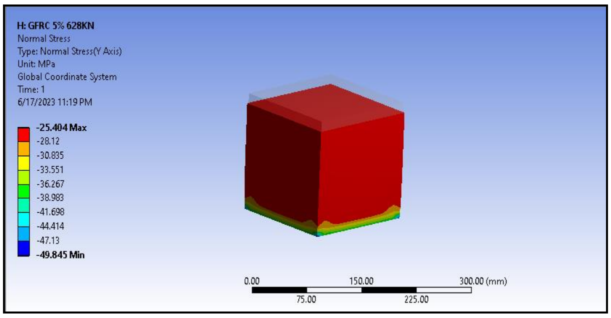

Fig. 22. Normal stress induced on GFRP specimen at 628kN load

The normal stress distribution plot is obtained for GFRP specimen at 628kN. The maximum normal stress obtained from the analysis is 25.404MPa as shown in figure 5.22.

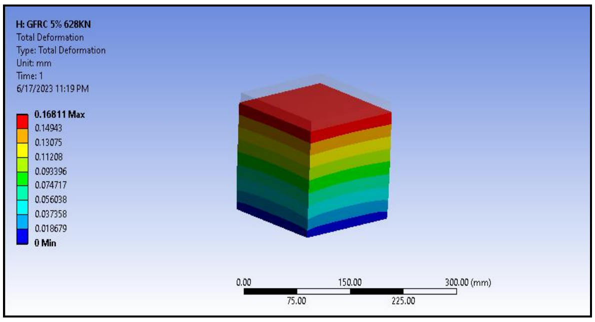

Fig. 23. Total deformation on induced on GFRP specimen at 628kN load

The maximum deformation obtained on GFRP specimen at 628kN is .168mm.

a) *Comparative analysis*

TABLE VIII. GLASS FIBER REINFORCED CONCRETE 3% GLASS FIBER CONTENT

Load	Normal Stress (MPa)
300kN	12.13
350kN	14.15
400kN	16.18
450kN	18.204
492kN	19.903

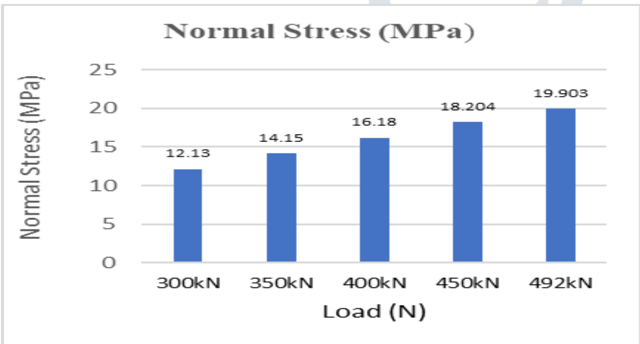

Fig. 24. Normal stress comparison at different loads for glass fiber reinforced concrete (3% fiber content)

TABLE IX. GLASS FIBER REINFORCED CONCRETE 5% GLASS FIBER CONTENT

Load	Normal Stress (MPa)
550kN	22.24
600kN	24.27
628kN	25.404

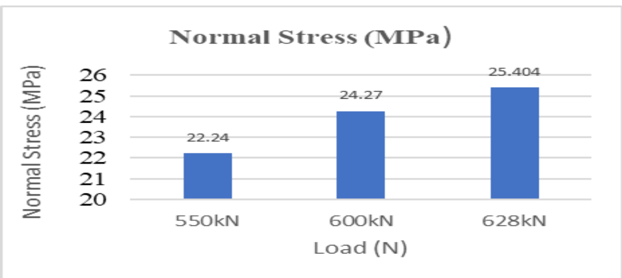

Fig. 25. Normal stress comparison at different loads for glass fiber reinforced concrete (5% fiber content)

V. CONCLUSION AND FUTURE WORK

After twenty years of intensive study, scientists are now comfortable saying that SCC can be used in a wide range of contexts. Both glass- and steel-fiber-reinforced concrete compressive strengths are calculated. SCC compressive strength increased with age. Compressive strength of concrete specimens exposed to heat variations was found to be significantly greater than that of specimens exposed to wet-dry and normal conditions. Finally, the compressive strength of the specimens exposed to wet-dry conditions was greater than that of the specimens exposed to normal conditions. Glass fibre reinforced concrete with a 0.3% fibre content has a compressive strength of 21.8N/mm2. When using a glass fibre content of 0.5 percent, the compressive strength of the resulting concrete is 27.9N/mm2.

The FEA simulation is conducted to determine the normal stresses and deformation of glass fiber specimen at different loads. From the FEA analysis on glass fiber specimen, the maximum normal stress obtained at 492kN is 19.903MPa. This is obtained for glass fiber percentage of 0.3%. The similar simulation was conducted for glass fiber reinforced concrete at different loads i.e. 550kN, 600kN, and 628kN. The maximum normal stress is obtained for concrete with 628kN load with magnitude of 25.404MPa

REFERENCES

[1] F. Aslani, G. Ma, D. L. Yim Wan, and G. Muselin, "Development of high-performance self-compacting concrete using waste recycled concrete aggregates and rubber granules," *J. Clean. Prod.*, 2018, doi: 10.1016/j.jclepro.2018.02.074.

[2] B. Djamila, B. Othmane, K. Said, and K. El-Hadj, "Combined effect of mineral admixture and curing temperature on mechanical behavior and porosity of SCC," *Adv. Concr. Constr.*, 2018, doi: 10.12989/acc.2018.6.1.069.

[3] Z. Keshavarz and H. Torkian, "Application of ANN and ANFIS Models in Determining Compressive Strength of Concrete," *J. Soft Comput. Civ. Eng.*, vol. 2, no. 1, pp. 62–70, 2018, doi: 10.22115/SCCE.2018.51114.

[4] M. H. Beigi, J. Berenjian, O. Lotfi Omran, A. Sadeghi Nik, and I. M. Nikbin, "An experimental survey on combined effects of fibers and nanosilica on the mechanical, rheological, and durability properties of self-compacting concrete," *Mater. Des.*, vol. 50, pp. 1019–1029, 2013, doi: 10.1016/j.matdes.2013.03.046.

[5] B. Alsubari, P. Shafigh, Z. Ibrahim, M. F. Alnahhal, and M. Z. Jumaat, "Properties of eco-friendly self-compacting concrete containing modified treated palm oil fuel ash," *Constr. Build. Mater.*, 2018, doi: 10.1016/j.conbuildmat.2017.09.174.

[6] P. G. Asteris, K. G. Kolovos, M. G. Douvika, and K. Roinos, "Prediction of self-compacting concrete strength using artificial neural networks," *Eur. J. Environ. Civ. Eng.*, 2016, doi: 10.1080/19648189.2016.1246693.